Aalto University School of Science and Technology
CFD-group/ Department of Applied Mechanics

MEMO No CFD/MECHA-20-2012 DATE: March 15, 2012

TITLE

The Effect of Free-Stream Turbulence Parameters on the SST $k-\omega$ Turbulence Model

AUTHOR(S)
Juhaveikko Ala-Juusela and Timo Siikonen

ABSTRACT

An assessment of the SST $k-\omega$ turbulence model is made using different free-stream values for k and ω. Flows over an ogive cylinder and the Onera M6 wing are used as test cases.

MAIN RESULT

It is found out that in some situations a solution is significantly affected by the free-stream turbulence quantities. A modification is made to the FINFLO code in order to remove the effect of the free-stream values.

PAGES
20

KEY WORDS
FINFLO, Fluent, CFD, turbulence, SST $k-\omega$

APPROVED BY

Timo Siikonen March 15, 2012

Contents

1 Introduction

In a recent study [1] it was found out that some values of the free-stream turbulence caused a friction factor to behave in a peculiar way, when the SST $k-\omega$ turbulence model [2, 3] is used. A similar behaviour has taken place in aerodynamic simulations. Usually the SST model works fine, but occasionally either no turbulence is generated or the result is clearly non-physical.

A problem in the free-stream values is that they are not based on real physical parameters, but are rather computational ones. It would be tempting to put zeros for the free-stream turbulence level as well as for the other variables. However, the definition of the turbulence viscosity is singular, as turbulence dissipation approaches zero. Furthermore, a production of turbulence is proportional to the eddy viscosity. Thus with a zero viscosity no turbulence is produced and one is calculating a laminar flow. By giving a suitably large value for the free-stream eddy viscosity, a turbulent flow may develop more rapidly during the iteration. Thus the free-stream values are by no means 'free' as they are given as input values.

On the basis of the previous studies it seems obvious that the implementation of the SST $k-\omega$ model to FINFLO is done in such a way that the model does not always work as expected. Two modifications to the implementation are suggested, and the first one is tested in this study. The effect of free stream values on the SST $k-\omega$-turbulence model is studied by simulating two different cases, a flow over an ogive cylinder and over the Onera M6 wing. In the simulations a set of different values for k and ω are applied. The first case is the same as calculated in Ref. [1]. In this study it is recalculated using FINFLO and Fluent codes, in order to compare the results obtained by different solvers.

In following, the turbulence model is firstly described, then simulation cases and grids are introduced and, finally, the results of the simulations are presented.

2 Flow Equations

A low-Reynolds number approach is used in FINFLO. The Reynolds-averaged Navier-Stokes equations, and the equations for the kinetic energy (k) and specific dissipation (ω) of turbulence can be written in the following form

$$\frac{\partial U}{\partial t}+\frac{\partial(F-F_v)}{\partial x}+\frac{\partial(G-G_v)}{\partial y}+\frac{\partial(H-H_v)}{\partial z}=Q \tag{1}$$

where the unknowns are $U=(\rho,\rho u,\rho v,\rho w,E,\rho k,\rho\omega)^T$. The inviscid fluxes are

$$F = \begin{pmatrix} \rho u \\ \rho u^2 + p + \frac{2}{3}\rho k \\ \rho v u \\ \rho w u \\ (E + p + \frac{2}{3}\rho k)u \\ \rho u k \\ \rho u \omega \end{pmatrix} G = \begin{pmatrix} \rho v \\ \rho u v \\ \rho v^2 + p + \frac{2}{3}\rho k \\ \rho w v \\ (E + p + \frac{2}{3}\rho k)v \\ \rho v k \\ \rho v \omega \end{pmatrix} H = \begin{pmatrix} \rho w \\ \rho u w \\ \rho v w \\ \rho w^2 + p + \frac{2}{3}\rho k \\ (E + p + \frac{2}{3}\rho k)w \\ \rho w k \\ \rho w \omega \end{pmatrix} \quad (2)$$

where ρ is the density, the velocity vector by using Cartesian components is $\vec{V} = u\vec{i} + v\vec{j} + w\vec{k}$, p is the pressure, k is the turbulent kinetic energy and ω its dissipation, and the total energy E is defined as

$$E = \rho e + \frac{\rho \vec{V} \cdot \vec{V}}{2} + \rho k \quad (3)$$

where e is the specific internal energy. The viscous fluxes are

$$F_v = \begin{pmatrix} 0 \\ \tau_{xx} \\ \tau_{xy} \\ \tau_{xz} \\ u\tau_{xx} + v\tau_{xy} + w\tau_{xz} - q_x \\ \mu_k(\partial k/\partial x) \\ \mu_\omega(\partial \omega/\partial x) \end{pmatrix} G_v = \begin{pmatrix} 0 \\ \tau_{xy} \\ \tau_{yy} \\ \tau_{yz} \\ u\tau_{xy} + v\tau_{yy} + w\tau_{yz} - q_y \\ \mu_k(\partial k/\partial y) \\ \mu_\omega(\partial \omega/\partial y) \end{pmatrix}$$

$$H_v = \begin{pmatrix} 0 \\ \tau_{xz} \\ \tau_{yz} \\ \tau_{zz} \\ u\tau_{xz} + v\tau_{yz} + w\tau_{zz} - q_z \\ \mu_k(\partial k/\partial z) \\ \mu_\omega(\partial \omega/\partial z) \end{pmatrix} \quad (4)$$

Here the stress tensor, τ_{ij}, includes laminar and turbulent components. The fluid is assumed to be Newtonian and, therefore, the laminar stresses are modelled by using Stokes hypothesis. The Reynolds stresses $\overline{\rho u_i'' u_j''}$ are included in the stress tensor τ_{ij}.

$$\tau_{ij} = \mu \left[\frac{\partial u_j}{\partial x_i} + \frac{\partial u_i}{\partial x_j} - \frac{2}{3}(\nabla \cdot \vec{V})\delta_{ij} \right] - \overline{\rho u_i'' u_j''} + \frac{2}{3}\rho k \delta_{ij} \quad (5)$$

For the Reynolds stresses, Boussinesq's approximation

$$-\overline{\rho u_i'' u_j''} = \mu_T \left[\frac{\partial u_j}{\partial x_i} + \frac{\partial u_i}{\partial x_j} - \frac{2}{3}(\nabla \cdot \vec{V})\delta_{ij} \right] - \frac{2}{3}\rho k \delta_{ij} \quad (6)$$

is utilized in RANS simulations. Here μ_T is a turbulent viscosity coefficient, which is calculated by using a turbulence model, and δ_{ij} is the Kronecker's

delta. In the momentum and energy equations, the kinetic energy contribution $2/3\rho k\delta_{ij}$ has been connected with pressure and appears in the convective fluxes, whereas the diffusive part is connected with the viscous fluxes. The viscous stresses contains a laminar and a turbulent parts. The heat flux can be written as

$$\vec{q} = -(\lambda + \lambda_T)\nabla T = -\left(\mu\frac{c_p}{Pr} + \mu_T\frac{c_p}{Pr_T}\right)\nabla T \tag{7}$$

where λ is a molecular and λ_T a turbulent thermal conductivity coefficient and Pr is a laminar and Pr_T a turbulent Prandtl number, and c_p is a specific heat at constant pressure. The diffusion of turbulence variables is modelled as

$$\mu_k\nabla k = \left(\mu + \frac{\mu_T}{\sigma_k}\right)\nabla k \tag{8}$$

$$\mu_\omega\nabla\omega = \left(\mu + \frac{\mu_T}{\sigma_\omega}\right)\nabla\omega \tag{9}$$

where σ_k and σ_ω are turbulent Schmidt numbers of k and ω, respectively. Density is obtained from an equation of state $\rho = \rho(p, T)$ Since the case for the ogive cylinder is incompressible, pressure differences $p - p_0$ are solved instead of pressure. The components of the source term Q are non-zero in possible buoyancy terms and in turbulence model equations.

In the present study both preconditioning and pressure correction methods are used to determine the pressure. The solution method applied is presented in [4], and the pressure correction method used is described in [5]. As compared to the traditional pressure correction methods, the basic difference of the present method is that all the residuals are calculated simultaneously and only once during an iteration cycle. The complexity of the coupled implicit solution is avoided by manipulating the explicit residuals. Since the same explicit stage is used as in preconditioning, the pressure correction can be used as a parallel solution method for the preconditioning.

In time-accurate simulations both precondition and pressure correction methods are used inside a physical time step [6]. Each time step is treated as a steady-state solution and iterations are made inside the time step. The time derivative term is treated as a source term. The method is fully implicit and a three-level second-order accurate approximation is used for the time derivative.

3 SST $k-\omega$ RANS-model

3.1 Basic Model

The model equations using an implicit summation over j-index are

$$\begin{aligned}\rho\frac{\partial k}{\partial t} + \rho u_j\frac{\partial k}{\partial x_j} &= P - \beta^*\rho k\omega \\ &+ \frac{\partial}{\partial x_j}\left[(\mu + \frac{\mu_T}{\sigma_k})\frac{\partial k}{\partial x_j}\right]\end{aligned} \tag{10}$$

$$\begin{aligned}\rho\frac{\partial\omega}{\partial t}+\rho u_j\frac{\partial\omega}{\partial x_j} &= \frac{\gamma\rho}{\mu_T}P-\beta\rho\omega^2 \\ &+ \frac{\partial}{\partial x_j}\left[(\mu+\frac{\mu_T}{\sigma_\omega})\frac{\partial\omega}{\partial x_j}\right] \\ &+ 2\rho\frac{1-F_1}{\sigma_{\omega 2}\omega}\frac{\partial k}{\partial x_j}\frac{\partial\omega}{\partial x_j}\end{aligned} \tag{11}$$

The model coefficients in Eqs. (10) and (11) are obtained from

$$(\sigma_k\ \sigma_\omega\ \beta)^T = F_1\,(\sigma_k\ \sigma_\omega\ \beta)_1^T + (1-F_1)\,(\sigma_k\ \sigma_\omega\ \beta)_2^T \tag{12}$$

with the following values

$$\begin{array}{lll}\sigma_{k1} = 1.176 & \sigma_{\omega 1} = 2.0 & \beta_1 = 0.075 \\ \sigma_{k2} = 1.0 & \sigma_{\omega 2} = 1.168 & \beta_2 = 0.0828\end{array}$$

Coefficients κ and β^* have constant values of 0.41 and 0.09. Coefficient γ is calculated from

$$\gamma = \frac{\beta}{\beta^*} - \frac{\kappa^2}{\sigma_\omega\sqrt{\beta^*}} \tag{13}$$

Term P in Eqs. (10) and (11) is the production of turbulent kinetic energy and calculated using the Boussinesq approximation from Eq. (6). The last term in the ω-equation originates from the transformed ϵ-equation and it is called a cross-diffusion term. The switching function which governs the choice between the ω- and the ϵ-equations is

$$F_1 = \tanh\left(\Gamma^4\right) \tag{14}$$

where

$$\Gamma = \min\left(\max\left(\frac{\sqrt{k}}{\beta^*\omega d};\frac{500\nu}{\omega d^2}\right);\frac{4\rho\sigma_{\omega 2}k}{CD_{k\omega}d^2}\right) \tag{15}$$

The first term is a turbulent length scale divided with the distance from the walls (d). This ratio is around 2.5 in a logarithmic layer and approaches zero in an outer layer. The second term has a value of ≥ 1 only in a viscous sublayer. The meaning of the third term is to ensure stable behaviour of F_1 when the value of ω in the free stream is small. It utilizes a parameter

$$CD_{k\omega} = \max\left(\frac{2\rho}{\sigma_{\omega 2}\omega}\frac{\partial k}{\partial x_j}\frac{\partial\omega}{\partial x_j};CD_{k\omega\,\min}\right) \tag{16}$$

which is a lower limit of the cross diffusion term. The main purpose of the switching function is to limit the use of the $k-\omega$ model into the boundary layer region. The switch is naturally a weak point in the model, but it seems to work at least in cases of external flows.

3.2 Modifications

On the basis of the sample calculations it was decided to change the relationships between the turbulence quantities. As a first trial the turbulence production terms are changed. In the simulations where wrong solutions have been obtained, the free-stream value of ω has been large. A simple and well known trick [7] to remove the effect of free-stream ω_∞ is to add a corresponding production on the right hand side of Eq. (10)

$$\beta^* \rho_\infty k_\infty \omega_\infty$$

As a result the free-stream turbulence never dies out as is the case without this term. In practice the evident decay is prevented by specifying a lower limit, i.e. the 'free-stream' value for the kinetic energy of turbulence. (In spite of the correction term this limitation is necessary in order to ensure a realizability of the model).

For the ω-equation a corresponding term is needed on the right-hand side of Eq. (11)

$$\beta \rho_\infty \omega_\infty^2$$

With these corrections k and ω behave realistically and the possibly large value of ω_∞ does not disturb the outer boundary layer. However, the turbulent viscosity remains unaffected and has a value specified via input. It is also possible to modify the equation for the eddy viscosity. In the SST model this is calculated from

$$\mu_T = \frac{a_1 \rho k}{\max\left(a_1 \omega, S F_2\right)} \tag{17}$$

where $a_1 = 0.31$ is Bradshaw's constant, $S = \sqrt{2 S_{ij} S_{ij}}$ is the absolute value of a strain rate tensor

$$S_{ij} = \frac{1}{2}\left(\frac{\partial u_i}{\partial x_j} + \frac{\partial u_j}{\partial x_i}\right) \tag{18}$$

and function F_2 is calculated from

$$F_2 = \tanh\left(\Gamma_2^2\right) \tag{19}$$

where

$$\Gamma_2 = \max\left(\frac{2\sqrt{k}}{\beta^* \omega d}; \frac{500\nu}{\omega d^2}\right) \tag{20}$$

In Ref. [7] the suggested values for the free-stream variables are $k_\infty = 1{\cdot}10^{-6} U_\infty^2$ and $\omega_\infty = 5U_\infty / L_{\mathrm{ref}}$. However, different sources suggest different values and at the moment the free-stream values are given in input case by case. In Ref. [8] the model constants have also been slightly modified by the original developer of the model. The effect of these changes is not yet studied in the present work.

A second method for removing the effect of a large background value of ω can be based on a modification of the viscosity formula. For a free stream

a suitable value for a maximum ω_∞ can be found on the basis of validation calculations. Since function F_2 is small outside the boundary layer, the eddy viscosity can be approximated as

$$\mu_{T,\infty} = \frac{\rho_\infty k_\infty}{\omega_0 + \omega_\infty} \tag{21}$$

Since k_∞ and $\mu_{T,\infty}$ are given via input and the upper limit for ω_∞ has the specified default value, parameter ω_0 can be solved. This parameter is applied throughout the computational domain, but only in connection with Eq. (17) and its influence is small in viscous regions. Thus a combination of $\mu_{T,\infty}$ and k_∞ does not lead to a large value of ω_∞, which seems to be the main cause of troubles with the SST-model.

4 Computational Domains, Grids and Boundary Conditions

4.1 Onera M6 wing

The Onera M6 wing is a swept, semi-span wing with no twist. It is based on a symmetric airfoil using the Onera D-section. A geometry of the wing is shown in Fig. 1 [9], where also pressure measurement taps are given.

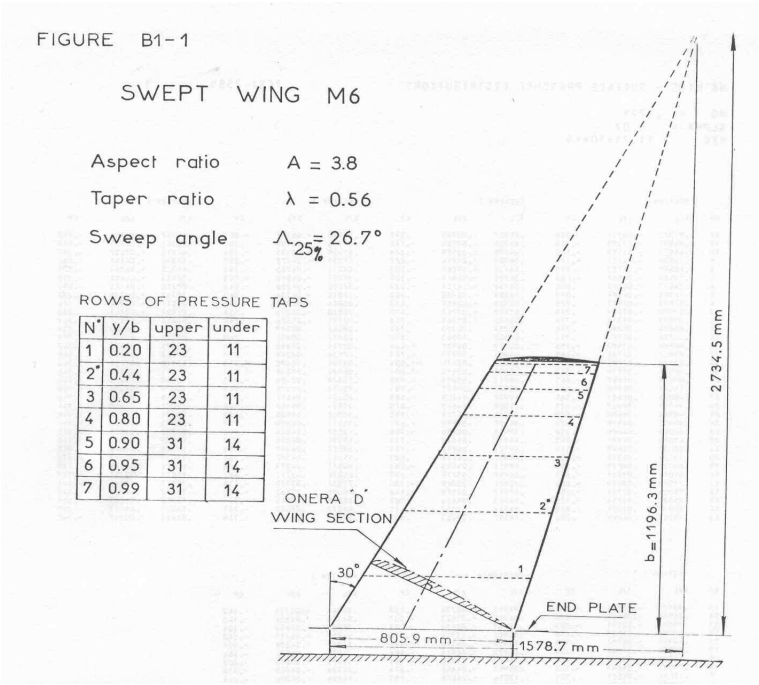

Fig. 1: Geometric layout of the Onera M6 wing [9].

A structured grid used in the simulations consists of four blocks and it has totally 1,572,864 cells. The surface grid and grid on a symmetry plane are shown in Fig. 2.

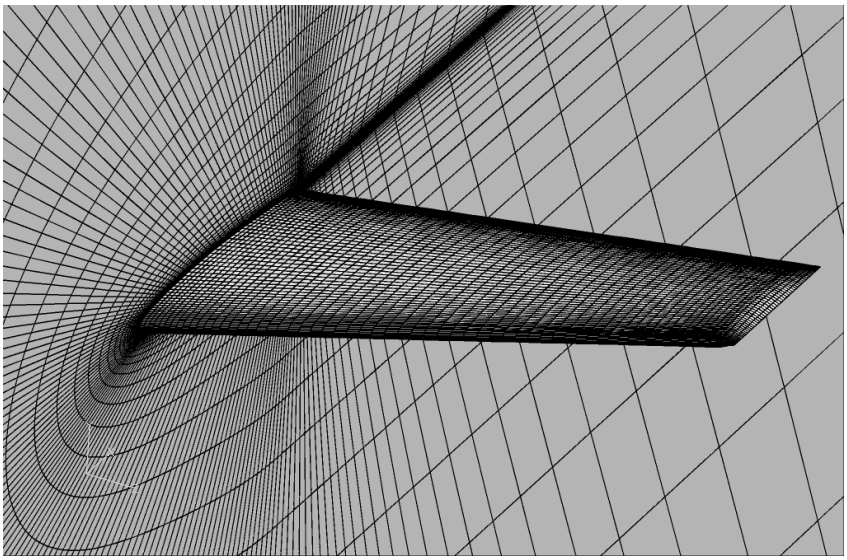

Fig. 2: Surface grid of the Onera M6 wing.

4.2 Ogive cylinder

This case is a hemispherical headed cylinder with a same head radius as a diameter of the straight cylindrical section. Geometry is shown in Fig. 3. In FINFLO simulation, a three degree sector of the cylinder is modelled. In Fluent simulation a two-dimensional grid is used. A structured grid applied consists of two blocks. On a cylinder there is a heavily clustered block with dimensions of 272 $\times$ 96 cells. An other block has 304 $\times$ 32 cells. A total number of the grid cells is 35,840. The computational grid is depicted in Fig. 4. Velocity and turbulence quantities are given at the inlet (left side in Fig. 4), pressure is given at the outlet and a symmetry boundary condition is used on the top surface. A singularity (or a pole in Fluent) is used as a boundary condition on the axis before the cylinder.

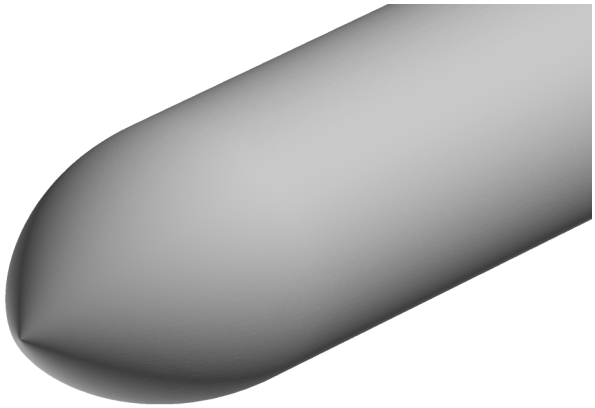

Fig. 3: Ogive cylinder.

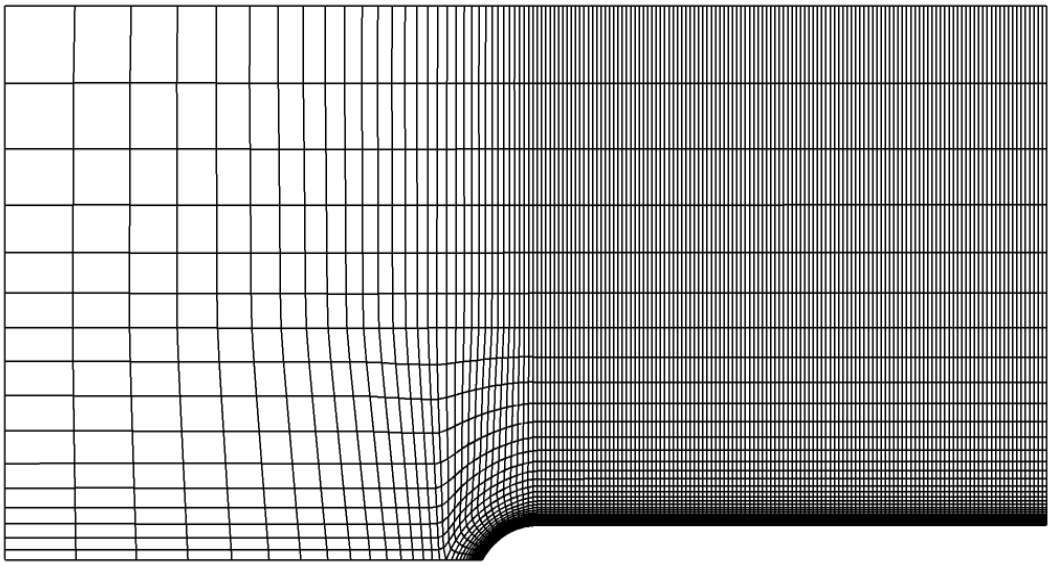

Fig. 4: Computational grid. Every second grid line is plotted.

5 Results

5.1 Onera M6 Wing

This case is simulated in order to test the SST k-ω turbulence model in a situation that resembles the flowfield around the wing of the Hornet fighter. The Mach number is 0.8395 and the angle of attack 3.06°. Free-stream values for the turbulence level (Tu) and the turbulent viscosity (μ_T/μ) are Tu=0.0001 and μ_T/μ=0.1 for case 1, Tu=0.0001 and μ_T/μ=0.01 for case 2, and Tu=0.00001 and μ_T/μ=0.01 for case 3, respectively.

Distributions of a pressure coefficient along the surface of the wing at cross sections y/b = 0.2, 0.44, 0.65, 0.8, 0.9 and 0.95 are shown in Fig. 5. Similar distributions of the friction coefficient are given in Fig. 6. One cannot detect differences between the cases from these curves. Minor differences can be seen, when comparing the corresponding data files. This irritating situation is typical, when a malfunction is searched, the model behaves perfectly.

In Fig. 7 distributions for the velocity and the turbulent kinetic energy at location s/c = 0.7 and z/b = 0.44 are shown. In Fig. 8 the corresponding distributions of specific dissipation rate ω and turbulent viscosity at same location are given. A shape and a thickness of the boundary layer are same with all cases of the free-stream turbulence values. The different free-stream levels are clearly visible, but those have an effect only on the eddy viscosity. That deviates somewhat in Case 2 on the outer edge of the boundary layer from the other results. However, the difference has no effect on the main variables.

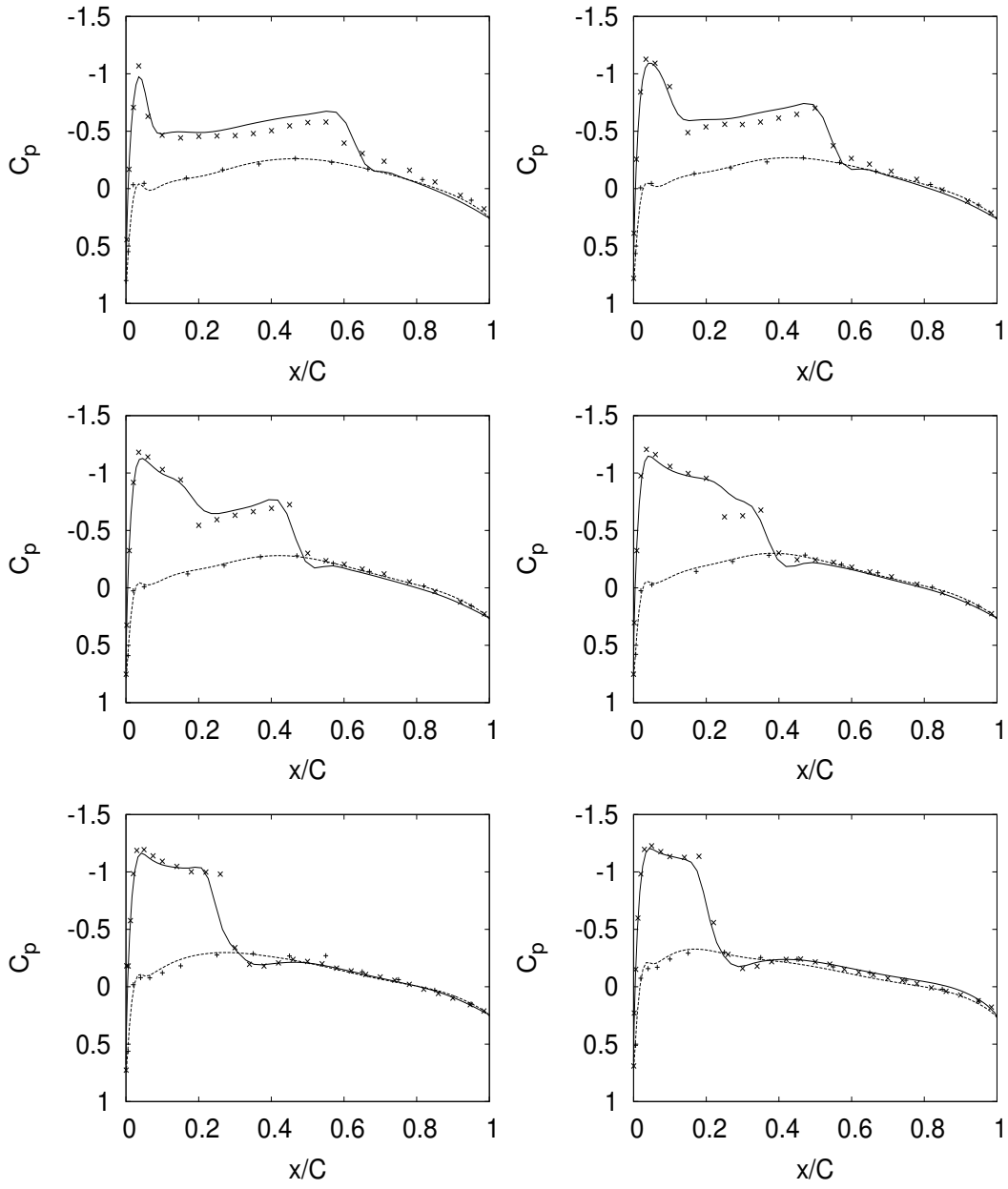

Fig. 5: Distributions of the pressure coefficient at cross sections $y/b = 0.2$, 0.44, 0.65, 0.8, 0.9 and 0.95

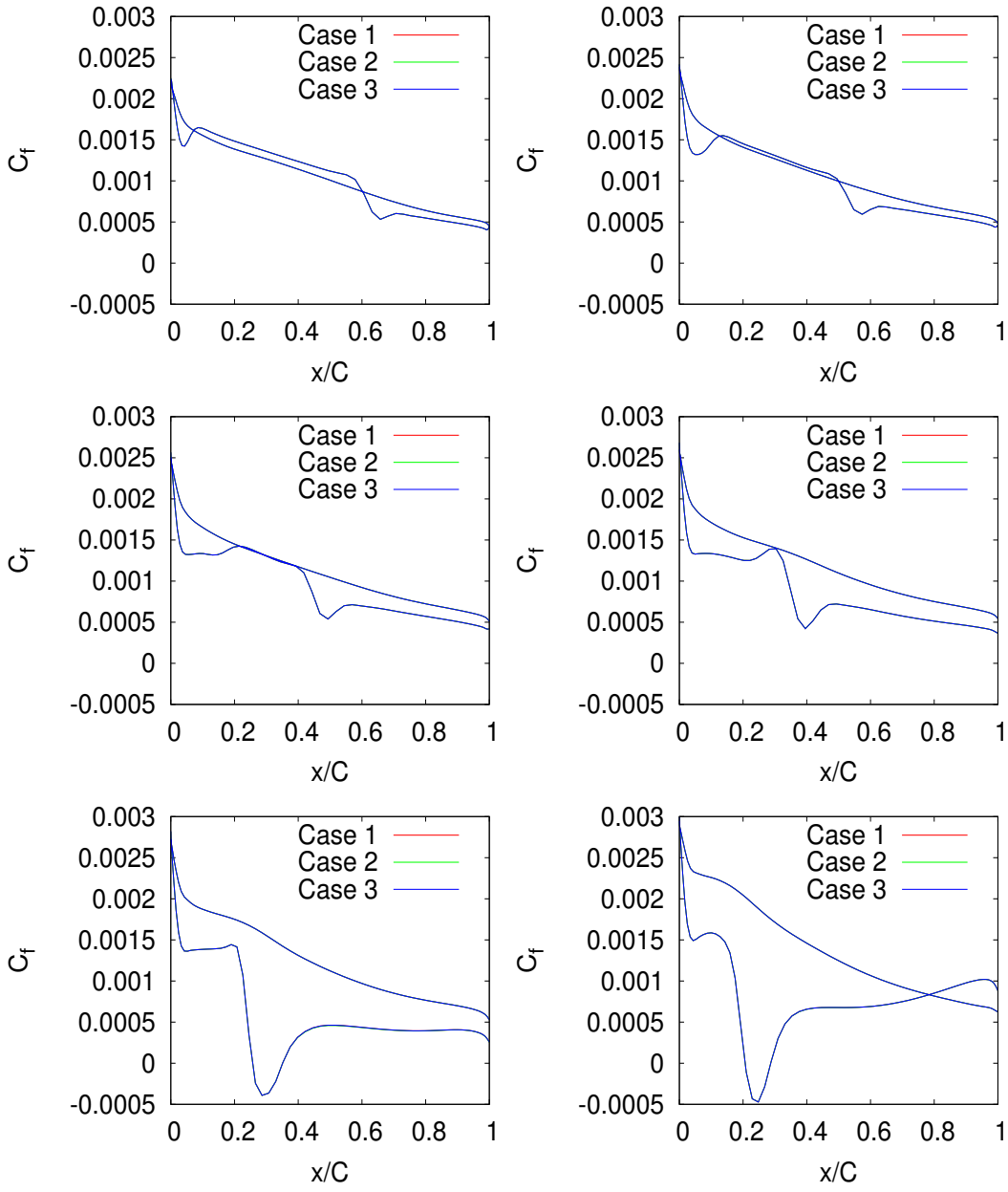

Fig. 6: Distributions of the friction coefficient at cross sections $y/b = 0.2$, 0.44, 0.65, 0.8, 0.9 and 0.95 on both sides of the M6 wing.

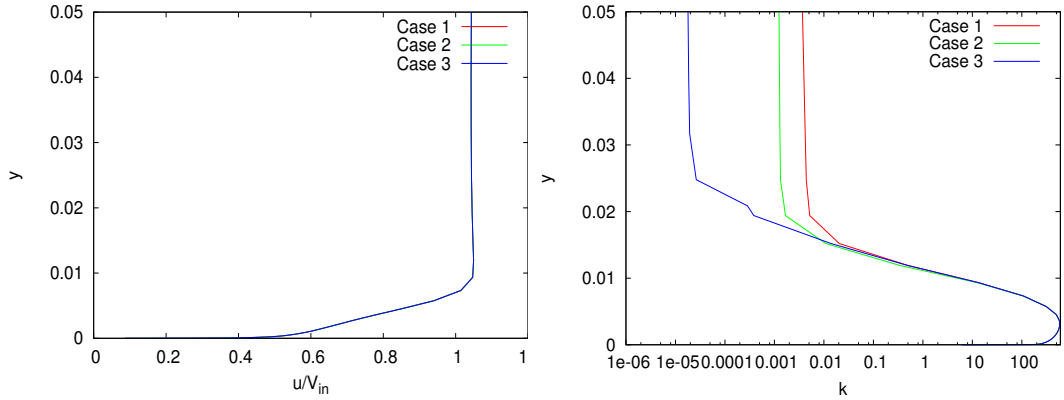

Fig. 7: Distributions of velocity and turbulent kinetic energy at location $s/c = 0.7$ and $z/b = 0.44$.

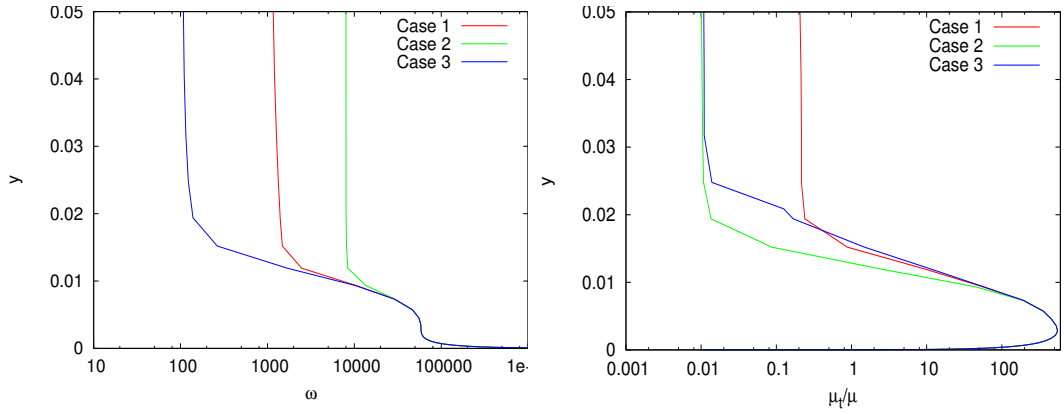

Fig. 8: Distributions of specific dissipation rate ω and turbulent viscosity at location $s/c = 0.7$ and $z/b = 0.44$.

5.2 Ogive Cylinder

In this study only the SST k-ω turbulence model is used for the ogive. In the earlier studies [1] a $k-\epsilon$ model produced expected results, whereas it was found out that the case is sensitive to the free-stream turbulence values, when the SST $k-\omega$ turbulence model is used. As an inflow boundary condition a velocity of 2.615 m/s is given. A Reynolds number based on the cylinder diameter is 136,500. The case is simulated with Fluent and FINFLO utilizing two different values for the free stream turbulence level (Tu) and the dimensionless turbulent viscosity (μ_T/μ). The values are Tu=0.001 and μ_T/μ=0.01 for the case referred as 'high values' and Tu=0.0002 and μ_T/μ=0.0002 for the case referred as 'low values'. The same values for the free stream turbulence level and turbulent viscosity were used in the previous study [1]. In addition, the case is simulated with FINFLO using zeroes as the free-stream values. Then the free-stream values are calculated from the default values built into the code. The values

for turbulent viscosity and intensity of turbulence are presented in Table 1. In this table RKLIM and OMEGALIM are FINFLO variables.

Table. 1: Simulated cases and parameters

Case	μ/μ_T	Tu	k_∞ (RKLIM)	ω_∞ (OMEGALIM)
Fluent k-w high FS turb	0.01	0.001		
Fluent k-w low FS turb	0.0002	0.0002		
Finflo k-w high FS turb	0.01	0.001	1.02E-02	5.73E+07
Finflo k-w low FS turb	0.0002	0.0002	4.10E-04	1.14E+08
Finflo k-w zero FS turb	0.	0.	4.67E-08	2615.0

Distributions of pressure and friction coefficients along the surface of the cylinder are shown in Fig. 9. Both high and low values with FINFLO code yield to a friction coefficient that decreases rapidly even though there is no corresponding change in geometry. In Fig. 10 distributions of velocity and turbulent kinetic energy at location $s/D = 5$, and in Fig. 11 the corresponding distributions of specific dissipation rate ω and the turbulent viscosity at the same location are shown. These figures show that in the FINFLO simulations using the low values, a shape of the velocity distribution and a thickness of the boundary layer are different from the other simulations.

After a few trials it was discovered that the solution is improved when the free-stream values are set to zero. This clearly indicates that a high value of ω_∞ might be a reason for the troubles encountered with the $k - \omega$ model. In this case only the first modification described (Eq. 17) is utilized. The results are shown in Figs. 9 - 11. Now the friction coefficient curve is smooth after a separation point and the boundary layers are equally thick in all simulations. There is a minor difference in the velocity distribution. Near the outer edge of the boundary layer in the Fluent results there is a sharp kink in the velocity profile, whereas the FINFLO result is smooth.

In the turbulence quantities the differences are more pronounced, but that does not matter if the influence on the main variables remain small. The low free-stream values are clearly visible on a logarithmic scale in Figs. 10 - 11. The largest difference is in the dimensionless eddy viscosity. In the FINFLO results the viscosity has a high value on the outer edge of the boundary layer, which is probably the reason for the smoother velocity profile there. The turbulence models contain many Schmidt numbers for a control of diffusion terms. There might be some differences between FINFLO and Fluent is these terms.

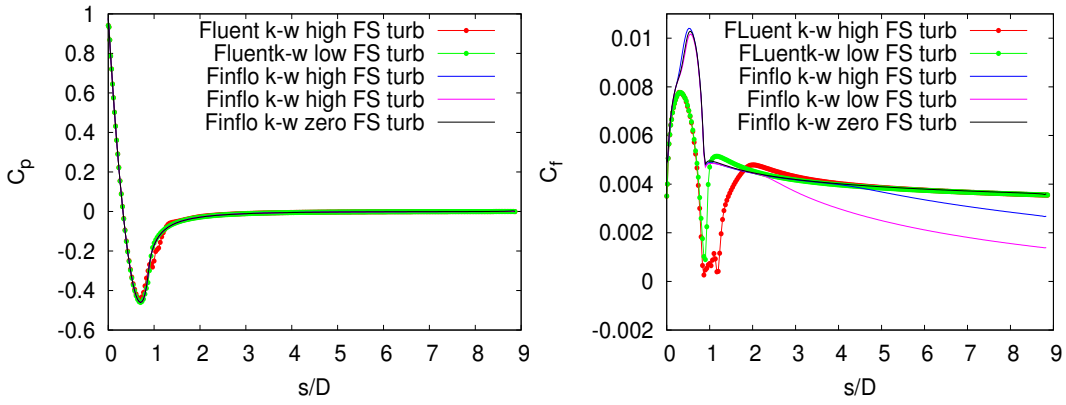

Fig. 9: Distributions of the pressure and the friction coefficients.

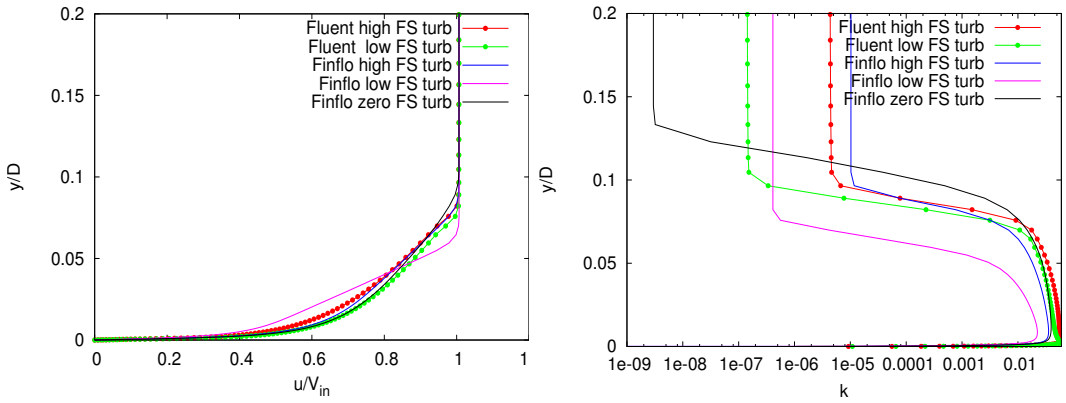

Fig. 10: Distributions of the velocity and the turbulent kinetic energy at location $s/D = 5$.

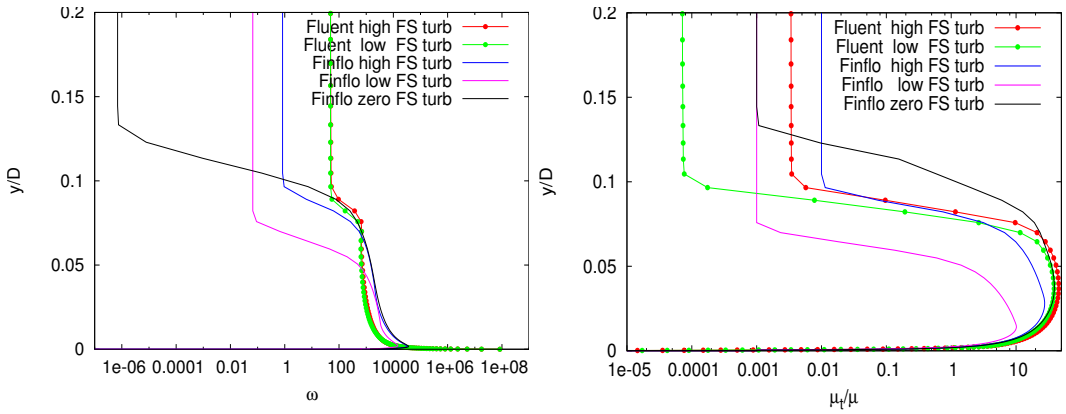

Fig. 11: Distributions of specific dissipation rate ω and the turbulent viscosity at location $s/D = 5$.

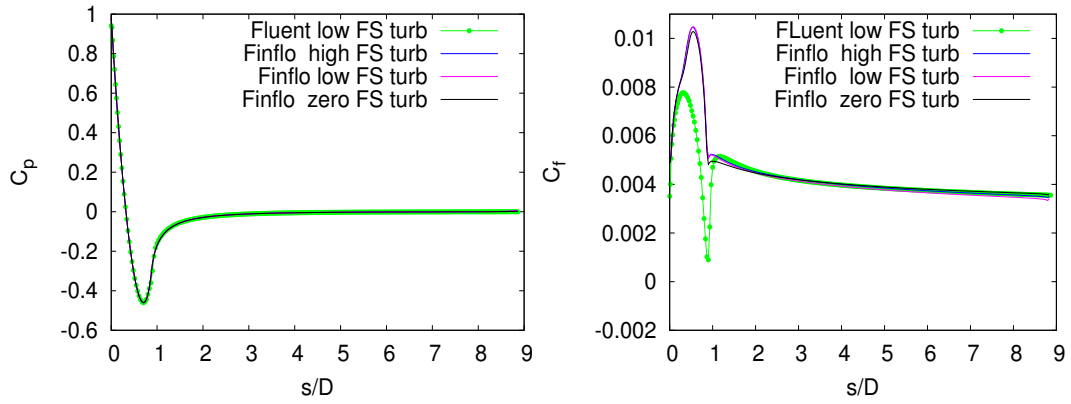

Fig. 12: Distributions of the pressure and the friction coefficients applying modification #1.

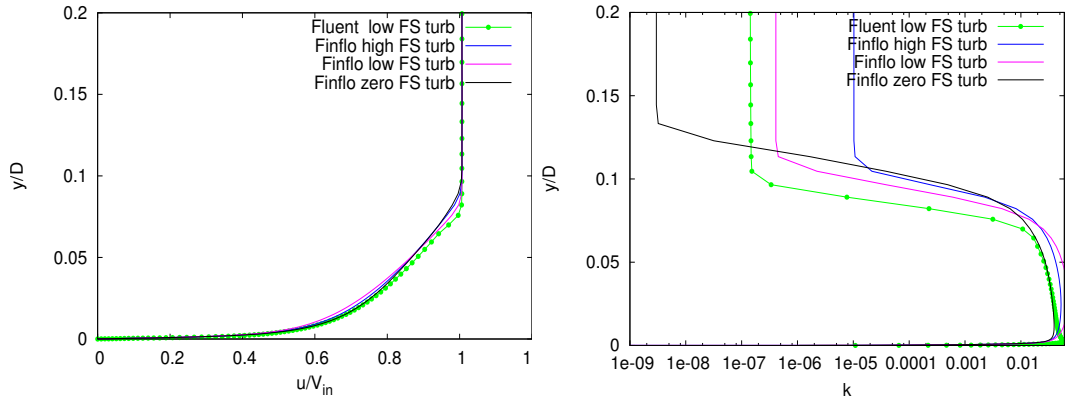

Fig. 13: Distributions of the velocity and the turbulent kinetic energy at location $s/D = 5$ applying modification #1.

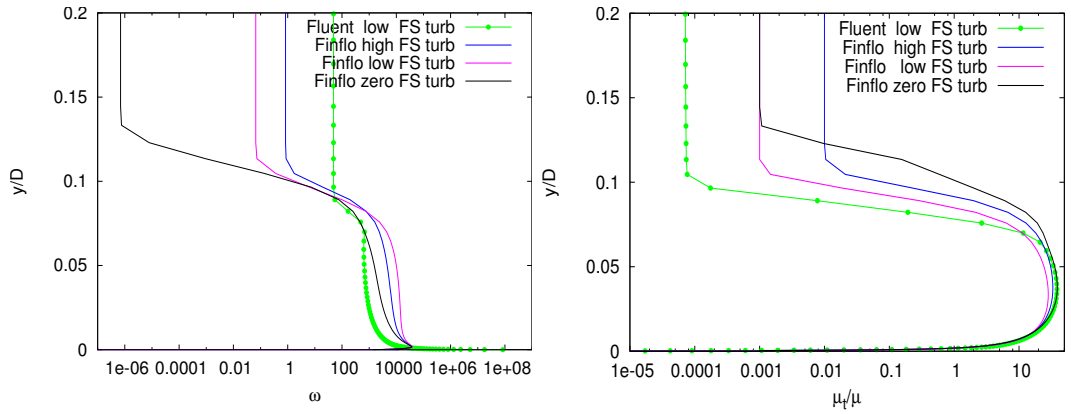

Fig. 14: Distributions of specific dissipation rate ω and the turbulent viscosity at location $s/D = 5$ applying modification #1.

6 Conclusions

In some simulations it has been found out that the free-stream values for the turbulence quantities may significantly effect the flow solution. Such a case, an ogive cylinder, is simulated in this study using both FINFLO and Fluent flow solvers. There is an anomaly in the FINFLO solution, which is not detected with the Fluent solution. A similar study of the free-stream turbulence quantities was done also for Onera M6 wing. In that case different values do not cause marked differences to the solution. It was noticed that there are such free stream values that give a proper solution for the ogive cylinder too. This leads to an observation that the free-stream values used with a traditionally utilized $k - \epsilon$ turbulence model are not always suitable for the SST $k - \omega$ turbulence model. A modification to the code was made, so that the user cannot accidentally apply unsuitable values, when the $k - \omega$ model is utilized. After the modification, all FINFLO simulations are in the line with the Fluent solution.

Although the modification seems to cure the problem, further testing is necessary, because even the original implementation usually gives good results. The modification is known in the literature as a SST-sust -model. That is in a way a new turbulence model in the SST family. There are many modifications suggested by various authors and it is somewhat difficult to establish a firm basis for the application of the model. The modification (SST-sust) tested in this work is now a default option in FINFLO that can be turned off via input. In the future the second modification should also be tested and reasonable default values should be given for the turbulence quantities. However, it should be noted that there are so many variations of the $k-\omega$ model that including all them as an option would not increase the reliability of the CFD simulations.

References

[1] Sipilä, T., "The Effect of Free-Stream Turbulence Parameters on a Flow over an Ogive Cylinder. Research Report VTT-R-08130-11.," VTT Technical Research Centre of Finland, Espoo, 2012.

[2] Menter, F., "Zonal Two Equation $k-\omega$ Turbulence Models for Aerodynamic Flows," in *24th AIAA Fluid Dynamics Conference*, AIAA, 1993. AIAA Paper 93–2906.

[3] Hellsten, A. and Laine, S., "Extension of the $k-\omega$-SST Turbulence Model for Flows over Rough Surfaces," in *1997 AIAA Atmospheric Flight Mechanics Conference*, (New Orleans, Louisiana), pp. 252–260, Aug 1997. AIAA Paper 97–3577–CP.

[4] Rahman, M., Rautaheimo, P., and Siikonen, T., "Numerical Study of Turbulent Heat Transfer from a Confined Impinging Jet Using a Pseudo-compressibility Method," in *Proceedings of the 2nd International Symposium on Turbulence, Heat and Mass Transfer*, (Delft), pp. 511–520, June 1997.

[5] Siikonen, T., "Developments in Pressure Correction Methods for a Single and Two Phase Flow CFD/MECHA-10-2010," Aalto University, Department of Applied Mechanics, 2010.

[6] Hoffren, J., "A Numerical Method for Simulating Unsteady Flow Including Solid/Fluid Interaction," Helsinki University of Technology, Laboratory of Aerodynamics, 1995. ISBN 951–22–2759–2.

[7] Spalart, P. and Rumsey, C. L., "Effective Inflow Conditions for Turbulence Models in Aerodynamic Calculations," *AIAA Journal*, Vol. 45, No. 10, 2007, pp. 2544–2553.

[8] Menter, F. R., Kuntz, M., and Langtry, R., "Ten Years of Industrial Experience with the SST Turbulence Model," in *Turbulence, Heat and Mass Transfer 4* (Hanjalic, K., Nagano, Y., and Tummers, M., eds.), pp. 625 – 632, Begell House, Inc., June 2003.

[9] Schmitt, V. and Charpin, F., "Pressure Distributions on the ONERA M6-Wing at Transonic Mach Number," in *AGARD-AR-138*, pp. B1–1 – B1–44, May 1979.